ACS OMEGA

http://pubs.acs.org/journal/acsodf

Article

Kinetic Effects of H_2O_2 Speciation on the Overall Peroxide Consumption at UO_2−Water Interfaces

Daniel Olsson,* Junyi Li, and Mats Jonsson

Cite This: https://doi.org/10.1021/acsomega.2c01048

Read Online

ACCESS | Metrics & More | Article Recommendations | Supporting Information

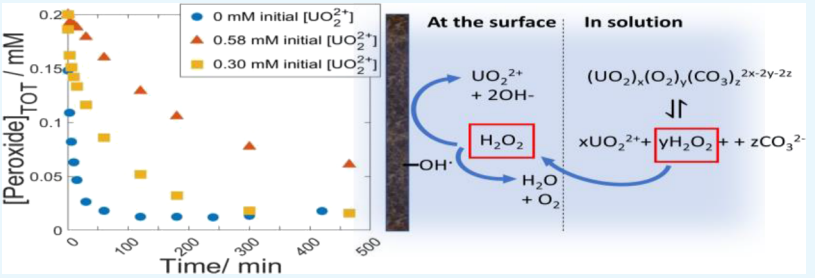

ABSTRACT: The interfacial radiation chemistry of UO_2 is of key importance in the development of models to predict the corrosion rate of spent nuclear fuel in contact with groundwater. Here, the oxidative dissolution of UO_2 induced by radiolytically produced H_2O_2 is of particular importance. The difficulty of fitting experimental data to simple first-order kinetics suggests that additional factors need to be considered when describing the surface reaction between H_2O_2 and UO_2. It has been known for some time that UO_2^{2+} forms stable uranyl peroxo-carbonato complexes in water containing H_2O_2 and HCO_3^-/CO_3^{2-}, yet this concept has largely been overlooked in studies where the oxidative dissolution of UO_2 is considered. In this work, we show that uranyl peroxo-carbonato complexes display little to no reactivity toward the solid UO_2 surface in 10 mM bicarbonate solution (pH 8−10). The rate of peroxide consumption and UO_2^{2+} dissolution will thus depend on the UO_2^{2+} concentration and becomes limited by the free H_2O_2 fraction. The rate of peroxide consumption and the subsequent UO_2^{2+} dissolution can be accurately predicted based on the first-order kinetics with respect to free H_2O_2, taking the initial H_2O_2 surface coverage into account.

1. INTRODUCTION

Uranium dioxide (UO_2) is the most common fuel material used in commercial nuclear reactors. While the unirradiated nuclear fuel has a low radioactivity, the formation of a small percentage of fission products and heavier actinides in the nuclear reactor leads to dramatically increased radioactivity that persists long after the fuel has been removed from the reactor.[1] Disposal of the spent nuclear fuel is one of the major challenges in nuclear technology. A solution that has been widely accepted is permanent storage in deep geological repositories.[2,3] In Sweden and Finland, the so-called KBS-3 concept will be applied, where the spent nuclear fuel is sealed in copper-coated cast iron canisters placed in the crystalline bedrock at a depth of around 500 m below the ground.[4] The canisters will be embedded in compacted bentonite clay. In the event of multiple barrier failure, the fuel would come in contact with groundwater. UO_2 has very low solubility in water but when oxidized into UO_2^{2+}, the solubility is enhanced by several orders of magnitude.[5,6] Complexation with carbonate (typically present in groundwater in concentrations 1−10 mM, depending on the geographical site of the repository)[7,8] increases the solubility further, favoring oxidative dissolution of the spent nuclear fuel matrix.[9] In general, the groundwater conditions at the depth of the repository are expected to be more reducing than oxidizing.[6] However, the intrinsic radioactivity of the spent nuclear fuel will induce groundwater radiolysis, resulting in the formation of reactive oxidants ($HO^\bullet$, $HO_2^\bullet$, and H_2O_2) and reductants (e_{aq}^-, $H^\bullet$, and H_2).[10−12] For kinetic reasons, the oxidants will dominate the surface reactions. It has been demonstrated that the radiolytic oxidant to which oxidative dissolution of UO_2-based fuel under repository conditions can mainly be attributed is H_2O_2.[13] Hydrogen peroxide has been shown to react with a UO_2 surface through the oxidation of U(IV) to U(VI) and catalytic decomposition on the oxide surface, leading to the formation of oxygen and water. The mechanisms can be described as follows:[14]

$$H_2O_2 + 2\,UO_2 \rightarrow 2\,(HO^\bullet - -UO_2) \quad (1)$$

$$HO^\bullet - -UO_2 \rightarrow OH^- + UO_2^+ \quad (2)$$

Received: February 21, 2022
Accepted: April 13, 2022

$$H_2O_2 + HO^{\bullet} - --UO_2 \rightarrow HO_2^{\bullet} + H_2O + UO_2 \quad (3)$$

$$HO_2^{\bullet} + HO_2^{\bullet} \rightarrow H_2O_2 + O_2 \quad (4)$$

Both reactions have the surface-bound hydroxyl radical as a common intermediate. In water containing $[HCO_3^-] > 1$ mM, the oxidative dissolution of UO_2 is limited by the one-electron oxidation described by reaction 2. For oxidative dissolution to occur, U(V) is further oxidized to U(VI). This could occur through a reaction with H_2O_2 or by disproportionation of two U(V) formed close to each other.

In systems with a high UO_2 surface area to solution volume ratio (SA/V), the kinetics of H_2O_2 consumption is expected to be first order with respect to H_2O_2 as the surface coverage is expected to become negligible. However, first-order fitting of experimental data has often resulted in low accuracy;[15,16] hence, the rate of consumption cannot be explained by strict first-order kinetics. The rate of H_2O_2 consumption at a given (measured) H_2O_2 concentration has been shown to be dependent on the initial H_2O_2 concentration, in sharp contrast to what is expected for first-order kinetics. This observation has previously been attributed to an irreversible alteration of the UO_2 surface, where it was shown that the reactivity of UO_2 pellets changed slightly over consecutive exposures.[17] However, there are other possible explanations that are yet to be explored.

It is well known that UO_2^{2+} forms stable uranyl-peroxo-carbonato complexes in solutions containing bicarbonate and hydrogen peroxide.[9,18−20] Several species have been identified, and the speciation of the system will depend on the concentrations of the solutes, ionic strength, and pH. In general, the equilibrium between a complex and uncomplexed peroxide can be described as follows:[20]

$$pUO_2^{2+} + qH_2O_2 + rCO_3^{2-} \rightleftarrows [(UO_2)_p(O_2)_q(CO_3)_r]^{2p-2q-2r} + 2qH^+ \quad (5)$$

Acid−base equilibria must also be accounted for to fully describe proton exchanges related to reaction (5). The pKa values for (HCO_3^-/CO_3^{2-}) and (H_2O_2/HO_2^-) are 10.34 and 11.75, respectively.[21,22]

Despite the fact that the existence of uranyl-peroxo-carbonato complexes has been known for quite some time, they have not been accounted for when discussing the kinetics and the mechanism of the reaction between H_2O_2 and UO_2. Instead, the peroxide concentrations measured in such systems are referred to as $[H_2O_2]$,[15] that is, free hydrogen peroxide. The equilibrium constants for the dominant complexes have been reported,[20,23] allowing for the simulation of the equilibrium concentrations of peroxide species based on thermodynamic stability. The uranyl-peroxo-carbonato complexes are negatively charged and are therefore expected to have a lower affinity toward the negatively charged UO_2 surface under alkaline conditions. Information regarding the reactivity of the peroxo-ligands in uranyl peroxo-carbonato complexes is limited. One of the few exceptions is a study by Chung et al.,[24] reporting decomposition rate constants for the complex $UO_2(O_2)(CO_3)_2^{4-}$ on various metal oxides.

In this work, we have experimentally explored the impact of H_2O_2-speciation on the kinetics and mechanism of H_2O_2-induced oxidative dissolution of UO_2 in aqueous systems by varying the initial UO_2^{2+} concentration. In addition, the impact of H_2O_2-speciation on the kinetics and mechanism of catalytic decomposition of H_2O_2 on ZrO_2 was studied in the same way. Speciation calculations have been employed in order to estimate the relative fractions of peroxide species at different stages of the reactions.

2. MATERIALS AND METHODS

2.1. Caution. Although the radioactivity of natural uranium (prior to its use in a nuclear reactor) is low, safety precautions regarding work with radioactive materials should be followed. Experiments involving uranium should only be conducted by trained staff and take place in facilities appropriate for the handling and storage of radioactive materials.

2.2. Exposures. The chemicals used throughout the experiments were of reagent grade or higher. All exposures were carried out in cylindrical glass vessels under N_2 purging, using 50 mg of UO_2 powder (supplied by Westinghouse Electric Sweden AB) in 30 mL of 10 mM bicarbonate solution (18.2 MΩ cm, Merck MilliQ). Sample volumes of 1 mL (or 2.5 if formaldehyde was analyzed) were removed from the reaction vessels at each point of measurements. The samples were filtered through 0.2 μm cellulose acetate syringe filters prior to analysis. The specific surface area of the powder had previously been determined as 4.6 ± 0.2 $m^2\ g^{-1}$, and the oxidation state was determined to be hyper stoichiometric $UO_{2.3}$.[15] Before exposure, the $UO_{2.3}$ powder was washed in 10 mM bicarbonate solution to remove preoxidized U(VI) from the surface. The washing process was carried out in five repetitions under N_2 purging, during which the solution was magnetically stirred for 5 min and replaced after sedimentation of $UO_{2.3}$, as indicated by a visibly clear solution. Before the replacement of the final washing solution with the solution used in the experiment, the uranyl concentration was measured to confirm uranyl from preoxidized U(VI) remained under the detection limit (<1 μM). The $UO_2^{2+}/H_2O_2/HCO_3^-(CO_3^{2-})$-solutions were prepared by dissolving various amounts of $UO_2(NO_3)_2 \times 6H_2O$ in washed $UO_{2.3}$ powder solutions (10 mM bicarbonate). Exposures were started as H_2O_2 was introduced to the systems.

Differences in the peroxide speciation at various concentrations of UO_2^{2+} were simulated using SPANA,[25] with ionic strength correction based on the Specific Ion-Interaction Theory (SIT) model.[5] The stability constants used in this work are the ones presented by Zanonato et al.[18] In a recent work, simulations based on the same set of constants were shown to be in good agreement with experimental observations using ^{13}C NMR under similar conditions (0.2 mM initial H_2O_2 in 10 mM HCO_3^-).[19]

2.3. Spectrophotometric Measurements with UV−vis. Concentrations of UO_2^{2+}, H_2O_2, and formaldehyde were measured with UV−vis absorption spectroscopy, using a Thermo Scientific Genesys 20 spectrophotometer. Uranyl concentrations were determined directly with the Arsenazo III method.[26,27] The absorbance of the U(VI)-(1,8-dihydroxy-naphthalene-3,6-disulphonic acid-2,7-bis[(azo-2)-phenylarsonic acid]) complex was measured at 653 nm. The reaction was carried out by mixing 60 μL 1 M HCl and 40 μL 16 wt % arsenazo-III reagent solution with 1.5 mL of diluted (100−200 μL) sample directly in the cuvette. H_2O_2 concentrations were determined indirectly with the Ghormley triiodide method,[28] by mixing 1.8 mL of diluted (100−200 μL) sample with 100 μL of 1 M potassium iodide and 100 μL of 1 M acetate/acetic acid buffer containing molybdate as a catalyst. The absorbance of I_3^- (formed in 1:1 ratio with reduced H_2O_2) was measured

https://doi.org/10.1021/acsomega.2c01048
ACS Omega XXXX, XXX, XXX−XXX

at 360 nm. It should be mentioned that the triiodide method was tested for solutions of various concentrations of UO_2^{2+} (0−4 mM). The measured concentration corresponded to the total amount of added H_2O_2 regardless of speciation. This is expected as the complex species will be converted back to H_2O_2 when the sample volumes are diluted in purified water (18.2 MΩ cm, Merck MilliQ) prior to measurement. The concentration measured with the triiodide method will henceforth be referred to as [peroxide], as to not be confused with the fraction of free H_2O_2 present in the UO_2 and ZrO_2 powder solutions during exposures.

The formation of surface-bound hydroxyl radicals following the decomposition of H_2O_2 on ZrO_2 was analyzed indirectly via the formation of formaldehyde (formed as one of the final products when tris(hydroxymethyl)aminomethane (Tris) is used as a radical scavenger). The produced formaldehyde was measured using a modified version of the Hantzsch reaction,[29] where formaldehyde reacts with acetoacetanilide and ammonia. Because of a larger sample volume required for the Hantzsch reaction than the 1 mL otherwise used, a volume of 2.5 mL sample was removed from the glass vessel for each point in time where concentrations were measured in the ZrO_2 powder solutions. The Hantzsch reaction was carried out in glass tubes by mixing 5 mL of 2 M ammonium acetate, 2 mL of 0.2 M acetoacetanilide, 2 mL of ethanol, and 1 mL of sample (filtered through 0.2 μm cellulose acetate filters). The reaction was carried out for 20 min in a heating bath at 313 K. The product, a dihydropyridine derivative, was measured at the absorbance maximum, occurring at 368 nm.[29]

3. RESULTS AND DISCUSSION

3.1. Effect of Speciation on the Consumption of H_2O_2 and UO_2^{2+} Dissolution. In order to vary the initial H_2O_2 speciation, experiments were performed using initial UO_2^{2+} concentrations of 0, 0.30, and 0.58 mM. These concentrations were selected based on thermodynamic calculations to correspond to initial free H_2O_2 fractions of 1, 0.5, and 0.1 based on the set conditions of 10 mM bicarbonate and the initial 0.2 mM H_2O_2. Total peroxide concentrations, dissolved UO_2^{2+} concentrations (i.e., total concentration with the initial concentration subtracted), and dissolution yields as functions of reaction time are presented in Figures 1, 2, and 3, respectively. Dissolution yields exceeding 100% are expected based on the hyperstoichiometric state of the powder. For $UO_{2.3}$, the dissolution yield would reach a maximum at ∼140% based on the already higher oxidation state of the uranium.

From Figure 1, it is clear that the rate of peroxide consumption is significantly reduced by the presence of uranyl in the solution. The rate decreases with increasing initial uranyl concentration. The same effect is observed for the rate of UO_2^{2+} dissolution shown in Figure 2. From the comparison of the dissolution yields in Figure 3, it is quite clear that the uranyl-peroxo-carbonato complexes have little or no influence on the final amount of UO_2^{2+} dissolved per amount of peroxide consumed, that is, the final dissolution yield is not affected by the initial presence of UO_2^{2+}. Fluctuations of the dissolution yield at low exposure times for 0.58 mM initial uranyl are expected as the result of uncertainties when measuring small changes to a relatively high total concentration. The yield becomes more certain as the dissolved amount increases. It should be noted that the dissolution yield depends on the total carbonate concentration. At total carbonate concentrations significantly below 10 mM, the dissolution yield will not reflect

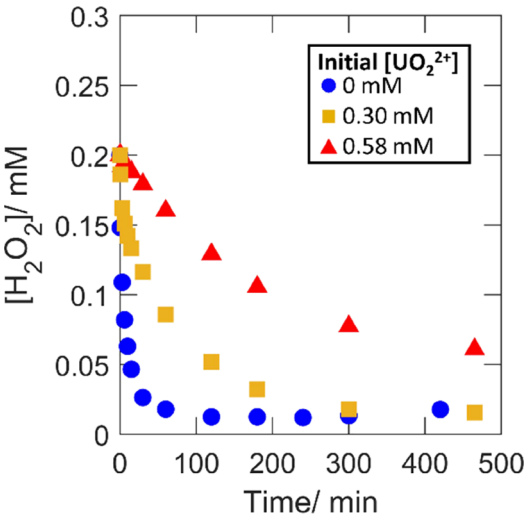

Figure 1. Peroxide concentrations as functions of exposure time for 50 mg of $UO_{2.3}$ powder in 30 mL of 10 mM HCO_3^- with 0.2 mM initial $[H_2O_2]$ and varied initial $[UO_2^{2+}]$.

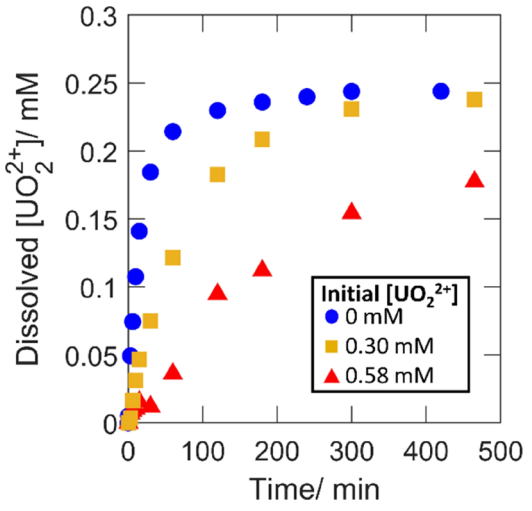

Figure 2. Dissolved UO_2^{2+} as functions of exposure time for 50 mg of $UO_{2.3}$ powder in 30 mL of 10 mM HCO_3^- with 0.2 mM initial $[H_2O_2]$ and varied initial $[UO_2^{2+}]$.

the competition between UO_2 oxidation by H_2O_2 and surface catalyzed decomposition of H_2O_2 but also be affected by limitations in the solubility of oxidized UO_2.

The observed suppression of the rates with added uranyl, along with the similar dissolution yields implies that the reaction mainly occurs between free H_2O_2 and the UO_2 surface. At higher initial UO_2^{2+} concentrations, the fraction of free H_2O_2 is lower, and therefore, the overall rates of peroxide consumption as well as UO_2^{2+} release are lower. Given the mechanism for the reaction between H_2O_2 and UO_2 (reactions 1−4), the presence of uranyl-peroxo-carbonato complexes would favor higher dissolution yields by decreasing the concentration of free H_2O_2. However, such a trend may not be possible to observe under these conditions because the dissolution yield is already at or near its maximum.

To analyze the speciation as a function of time in the three experiments, we simulated the thermodynamic equilibrium concentrations of the dominant peroxide species as functions of exposure times using SPANA. pH was measured at the start

https://doi.org/10.1021/acsomega.2c01048
ACS Omega XXXX, XXX, XXX−XXX

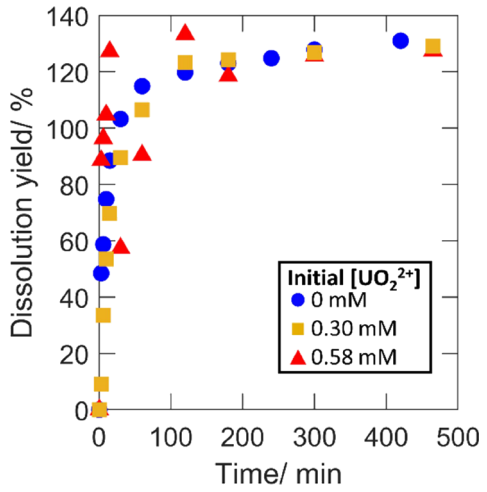

Figure 3. Cumulative dissolution yields as functions of exposure time for 50 mg of $UO_{2.3}$ powder in 30 mL of 10 mM HCO_3^- with 0.2 mM initial $[H_2O_2]$ and varied initial $[UO_2^{2+}]$.

and at the end of each exposure, and the average (~pH 9) was assumed when performing the simulations. The simulated concentrations for 0.2 mM initial H_2O_2 and 0, 0.30, and 0.58 mM initial $[UO_2^{2+}]$ are presented in Figure 4a–c, respectively.

As can be seen in Figure 4 a, the dominating peroxide species in the case where no UO_2^{2+} is added is initially free H_2O_2 while in the cases where the initial $[UO_2^{2+}]$ exceeds 0.3 mM (Figure 4b,c), the peroxide is expected to predominantly exist in the form of $(UO_2)_2(O_2)(CO_3)_4^{6-}$. The fraction of free H_2O_2 decreasing with increasing initial UO_2^{2+} is in qualitative agreement with the conclusion above that the reaction occurs between free H_2O_2 and UO_2 as reflected by the relative rates.

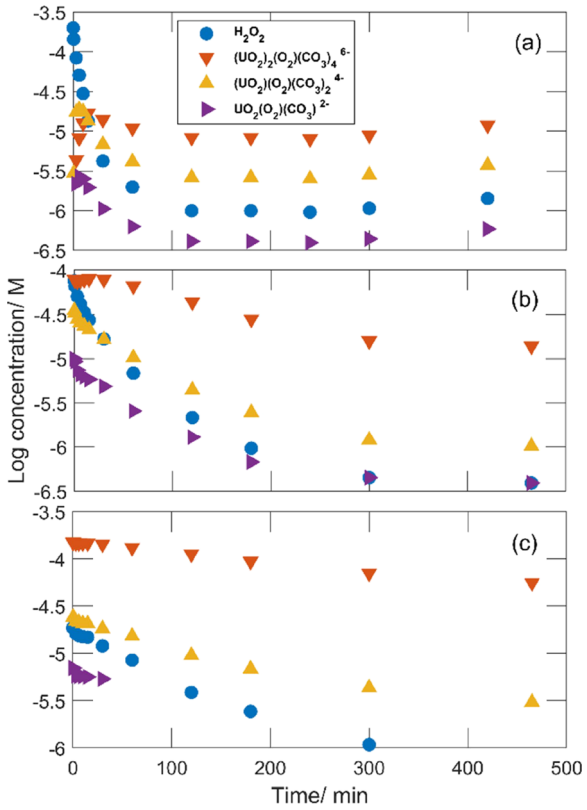

Figure 4. Simulations of the log equilibrium concentrations for the dominant peroxide species as functions of exposure time in 10 mM bicarbonate solutions containing 0.2 mM H_2O_2 and 0 mM (a), 0.3 mM (b), and 0.6 mM (c) UO_2^{2+} at the start of the exposure. The calculations were performed using concentrations presented in Figures 1 and 2 and pH 9.2.

3.2. Kinetic Analysis of Reference Experiments with Varied Initial $[H_2O_2]$. To quantitatively explore the concept of nonreactive peroxo-complexes, we analyzed the kinetics of peroxide consumption for a set of previously published data.[15] The data set includes H_2O_2 and UO_2^{2+} concentrations as functions of reaction time for $UO_{2.3}$ powder in 10 mM HCO_3^- solutions, exposed to 0.2, 0.5, 1.0, and 2.0 mM initial H_2O_2 concentrations. It was found that the peroxide consumption rate at a given peroxide concentration varied significantly depending on the initial concentration of H_2O_2. The proposed explanation in the original work is an alteration of the reactive interface, leading to a change in reactivity.[15] Here, we consider overestimations of free H_2O_2 available to the UO_2 surface as a plausible explanation for this observation as the total peroxide measured was thought to exclusively be in the form of H_2O_2. A comparison of the calculated free H_2O_2 vs the total peroxide concentration is presented in Figure 5. The concentration of free H_2O_2 is based on speciation calculations using the reported UO_2^{2+} and total peroxide concentrations (measured with the triiodide method).[15]

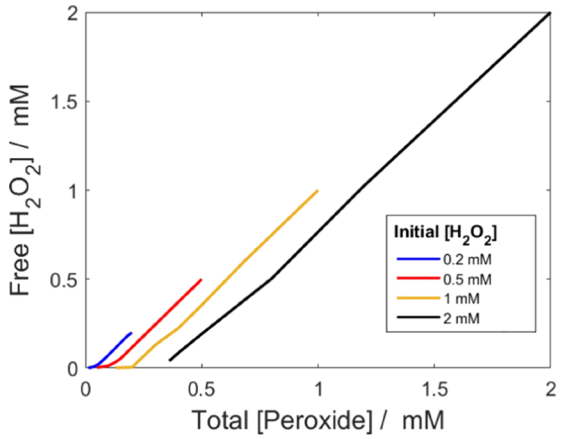

Figure 5. Calculated free H_2O_2 concentration as a function of the total peroxide concentration for $UO_{2.3}$ powder in 10 mM HCO_3^-, with varied initial H_2O_2 concentrations. Calculations were based on the reported uranyl and peroxide concentrations (see reference, Figure 1)[15] and an assumed pH 9.

In Figure 5, it is clear that the H_2O_2 available to the surface at a given measured peroxide concentration is expected to vary based on the initial H_2O_2 (i.e., on the amount of dissolved UO_2^{2+}). It is interesting to note that the expected effect is a parallel shift of the curves in Figure 5, to which the consumption rate would correspond given first-order kinetics with respect to the fraction of free H_2O_2.

Although the parallel shift attributed to speciation could account for part of the experimental observation, it is obvious that it is not the only reason. Assuming the rate of H_2O_2 consumption to be directly proportional to the concentration of free H_2O_2, a plot of the rate as a function of total peroxide concentration would look like that given in Figure 5. However, in the original work, it is quite clear that the slopes of the

https://doi.org/10.1021/acsomega.2c01048
ACS Omega XXXX, XXX, XXX−XXX

individual curves (for each initial H_2O_2 concentration) differ from each other (the slopes decrease with increasing initial H_2O_2 concentration).

Differences in pH would be one possible reason for the difference in slopes. Simulations of the speciation for the systems containing 0.2 and 2 mM initial H_2O_2 at various pH suggest that the slopes of $[H_2O_2]$ vs [peroxide] (presented in Figure 7) would decrease slightly with increasing pH within the pH range 7−11 (see Tables S1−S4 in the Supporting Information for comparison). In general, we have observed a slight increase in pH as the reaction progresses but not to the extent that would explain the observed differences in slopes.

In the original work, it was demonstrated that the initial rate of H_2O_2 consumption depends on the initial H_2O_2 concentration through a relationship that can be given by a Freundlich adsorption isotherm. This suggested that the initial H_2O_2 consumption rate is proportional to the surface density of adsorbed H_2O_2. In order to model the kinetics of the system taking into account that the rate constant for the reaction between H_2O_2 and the surface displays some dependence on the initial H_2O_2 concentration, we determined the initial rate of H_2O_2 consumption from the derivative of the multi-exponential function obtained from the fitting to experimental data. The first order rate constant to be used in the simulation was then derived by dividing the initial rate with the initial H_2O_2 concentration. The resulting rate constants are listed in the Supporting Information (see Table S5). By multiplying the free H_2O_2 concentrations derived from the speciation calculation (Figure 5) with the calculated rate constants, we obtain the expected rates of peroxide consumption. For comparison, both the calculated rates and the experimentally determined rates for the reference experiment where the initial H_2O_2 concentration was varied are plotted in Figure 6a.

A similar plot is shown in Figure 6b for the data set where the initial uranyl concentration was varied (data presented in Figures 123). It should be noted that the SA/V is higher in these systems. Hence, the first-order rate constants derived for the first set of experiments cannot be used here. The higher SA/V also results in larger initial drops in peroxide concentration because of the fast adsorption of H_2O_2. This has a significant impact on the fitting of the peroxide concentration over exposure time. For this reason, the initial point has been excluded when fitting the data to improve the overall fit. Because two of the systems shown in Figure 6b has a significant amount of the peroxide in various uranyl-peroxo-carbonato complexes the first-order rate constants were calculated as the consumption rate divided by the calculated free $[H_2O_2]$ after the initial rapid adsorption step.

As can be seen in Figure 6a, the calculated rates based on first-order kinetics with respect to the fraction of free H_2O_2 are in very good agreement with the experimental data when the pseudo first-order rate constants are calculated separately. This implies that both H_2O_2 speciation and the adsorption dependent pseudo first-order rate constant must be accounted for when describing the kinetics of H_2O_2 consumption on UO_2.

Notably, there is less agreement between the experimental rates and the rates based on speciation calculations for the 2 mM initial H_2O_2 exposure compared to the exposures at lower initial H_2O_2 concentrations. In addition, the experimental rate has a dependence on the peroxide concentration different from that of the lower exposures as the rate appears to reach zero with a significant amount of peroxide remaining in solution.

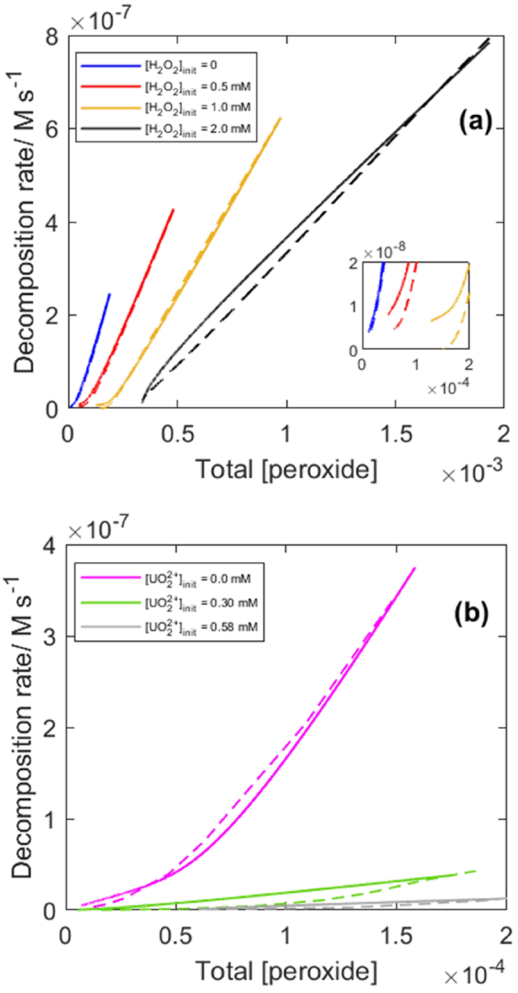

Figure 6. Comparisons of calculated rates based on first-order kinetics with respect to free $[H_2O_2]$ (dashed lines) and the rates obtained by exponential fitting of the raw data for (a) a reference data set with varied initial $[H_2O_2]$, SA/V = 5400 m^{-1} and (b) a set with varied initial $[UO_2^{2+}]$, SA/V = 9000 m^{-1}.

This could be a problem related to the fitting of the experimental data as the fit largely relies on the last point of the measured [peroxide] (see Figure S1d).

In general, the rates estimated on the basis of speciation calculations and first-order rate constants appear to be lower than the experimental rates in cases where the fraction of free H_2O_2 is low as can be seen toward the end of the exposure with lower initial H_2O_2 concentration (see the scale-up in Figure 6a). Underestimated rates are also obtained as the reaction progresses for the two cases where uranyl was added prior to exposure, as can be seen in Figure 6b (a scale-up is available as Supporting Information, see Figure S6). This could be attributed to uncertainties in the stability constants used for the speciation calculations. The calculated relative fractions are sensitive to uncertainties in the stability constants, as was demonstrated by Zanonato et al.[20]

3.3. Effects of Uranyl Peroxo-Carbonato Speciation on the Decomposition of H_2O_2 on ZrO_2. H_2O_2 reacts with ZrO_2 by catalytic decomposition only. The ZrO_2 system is therefore very suitable for studying the effect of H_2O_2 speciation on surface-catalyzed decomposition of H_2O_2. It has been shown in several relatively recent studies[30−33] that the surface-bound hydroxyl radical is formed also in the catalytic

https://doi.org/10.1021/acsomega.2c01048
ACS Omega XXXX, XXX, XXX−XXX

decomposition of H_2O_2 on ZrO_2. This has been demonstrated by using various radical scavengers. One of them is tris(hydroxymethyl)aminomethane (Tris), which produces formaldehyde upon reaction with the hydroxyl radical.[34] Formaldehyde can readily be detected and thereby probe the accumulated hydroxyl radical production. Two sets of experiments were performed. In the first set, the H_2O_2/HCO_3^-(CO_3^{2-})/ZrO_2 system was investigated with and without Tris, and in the second set, the same systems with initially added UO_2^{2+} were investigated. The peroxide concentrations ([H_2O_2] in the absence of UO_2^{2+}) as functions of exposure time are presented in Figure 7.

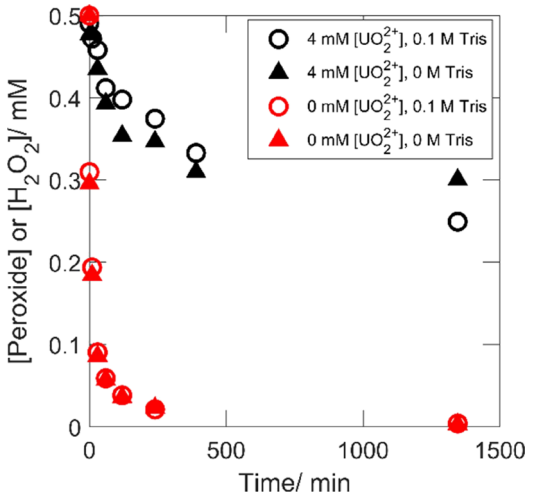

Figure 7. Total [peroxide] ([H_2O_2] in the absence of U (red keys)) as functions of exposure time for ZrO_2 powder in 0.1 M HCO_3^- with 0.5 mM H_2O_2, 0.1 M/ 0 M Tris and 4 mM/0 mM [UO_2^{2+}].

As can be seen in Figure 7, H_2O_2 is rapidly consumed in the absence of UO_2^{2+}, and the presence of Tris does not appear to influence the rate at which H_2O_2 is consumed on ZrO_2. The presence of UO_2^{2+} clearly has a significant suppressing effect on the kinetics of peroxide consumption on ZrO_2 where catalytic decomposition is the only reaction path. After 22 h and 26 min when the last measurement was made, approximately half of the peroxide had been consumed. The detected formaldehyde in the presence and absence of UO_2^{2+} as functions of exposure time is presented in Figure 8.

The detection of formaldehyde in Figure 8 indicates the formation of surface-bound hydroxyl radicals in the presence and absence of UO_2^{2+} that continues to be scavenged by Tris also after most of the H_2O_2 has been consumed. Interestingly, the final formaldehyde yields appear similar for the two sets because roughly twice as much formaldehyde was detected in the absence of UO_2^{2+}, where twice the amount of H_2O_2 was converted. Hence, the reaction mechanism would appear to be the same involving the formation of surface-bound hydroxyl radicals. Again, this would imply that the reaction proceeds via the fraction of free H_2O_2 and that the complexes merely act as a sink for free H_2O_2.

4. CONCLUSIONS

The formation of uranyl peroxo-carbonato complexes suppresses the rate of peroxide consumption by acting as temporary sinks for H_2O_2 while surface reactions on UO_2 and ZrO_2 likely proceed via the fraction of free H_2O_2. The peroxide

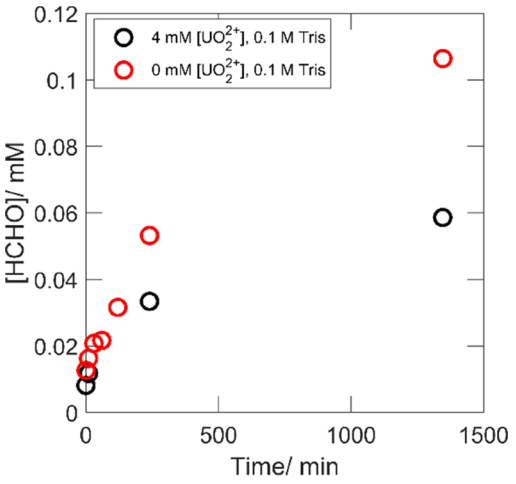

Figure 8. Detected formaldehyde as functions of exposure time in the presence and absence of 4 mM UO_2^{2+} with 0.1 M Tris as an OH-radical scavenger.

in the various complex forms present in 10 mM bicarbonate show little or no reactivity toward the UO_2 and ZrO_2 surfaces under alkaline conditions (pH 8−10), as supported by the similar dissolution yields and the ratio between scavenged OH-radicals and the amount of consumed peroxide, regardless of the speciation. The very low reactivity of the complexes can largely be attributed to the electrostatic repulsion between the negatively charged complexes and the negatively charged surface. The kinetics of H_2O_2 consumption on UO_2 surfaces in HCO_3^- containing aqueous systems can be correctly reproduced using the fraction of free H_2O_2 determined from speciation calculations and the pseudo first-order rate constant given by the Freundlich isotherm for H_2O_2 on UO_2.

■ ASSOCIATED CONTENT

Supporting Information

The Supporting Information is available free of charge at https://pubs.acs.org/doi/10.1021/acsomega.2c01048.

Fittings of [peroxide] vs time data to multi-exponential equations (Figures S1 and S2), consumption rates vs time (Figure S3), consumption rates vs [peroxide] (Figure S4), measured uranyl concentrations vs exposure times related to the dissolution presented in Figure 2 (Figure S5), scale-up of Figure 6b (Figure S6), calibration data for the Arsenazo-III method (Figure S7), speciation calculation data for pH 7, 8, 9, 10, and 11 (Tables S1−S4), and pseudo first-order rate constants used for calculations of the rates shown in Figure 8 (listed in Table S5) (PDF)

■ AUTHOR INFORMATION

Corresponding Author

Daniel Olsson − *Department of Chemistry, KTH Royal Institute of Technology, Stockholm SE-100 44, Sweden;* orcid.org/0000-0002-5167-0202; Phone: +46 72 316 29 39; Email: daniols@kth.se

Authors

Junyi Li − *Department of Chemistry, KTH Royal Institute of Technology, Stockholm SE-100 44, Sweden*

https://doi.org/10.1021/acsomega.2c01048
ACS Omega XXXX, XXX, XXX−XXX

Mats Jonsson − *Department of Chemistry, KTH Royal Institute of Technology, Stockholm SE-100 44, Sweden;* orcid.org/0000-0003-0663-0751

Complete contact information is available at: https://pubs.acs.org/10.1021/acsomega.2c01048

Notes

The authors declare no competing financial interest.

■ ACKNOWLEDGMENTS

This work was financially supported by the Swedish Nuclear Fuel and Waste Management Company (SKB) and the China Scholarship Council (CSC).

■ REFERENCES

(1) Verma, V. K.; Katovsky, K. Spent Nuclear Fuel and Alternative Methods of Transmutation. In *Spent Nuclear Fuel and Accelerator-Driven Subcritical Systems*; Springer: Singapore, 2019; pp 1−19.

(2) Puranen, A.; Barreiro, A.; Evins, L. Z.; Spahiu, K. Spent fuel corrosion and the impact of iron corrosion − The effect of hydrogen generation and formation of iron corrosion products. *J. Nucl. Mater.* **2020**, *542*, No. 152423.

(3) Faybishenko, B.; Birkholzer, J.; Sassani, D.; Swift, P. *International Approaches for Nuclear Waste Disposal in Geological Formations: Geological Challenges in Radioactive Waste Isolation—Fifth Worldwide Review*, 2017.

(4) Sellin, P.; Leupin, O. X. The Use of Clay as an Engineered Barrier in Radioactive-Waste Management − A Review. *Clays Clay Miner.* **2013**, *61*, 477−498.

(5) Brönsted, J. N. Studies on solubility. IV. The principle of the specific interaction of ions. *J. Am. Chem. Soc.* **1922**, *44*, 877−898.

(6) Kertes, A. S.; Guillaumont, R. Solubility of UO_2. A comparative review. *Nucl. Chem. Waste Manage.* **1985**, *5*, 215−219.

(7) King, F.; Ahonen, L.; Taxén, C.; Vuorinen, U.; Werme, L. *Copper corrosion under expected conditions in a deep geological repository*; Swedish Nuclear Fuel and Waste Management Co (SKB): Stockholm, 2001.

(8) Somervuori, M.; Isotahdon, E.; Nuppunen-Puputti, M.; Bomberg, M.; Carpén, L.; Rajala, P. A Comparison of Different Natural Groundwaters from Repository Sites—Corrosivity, Chemistry and Microbial Community. *Corros. Mater. Degrad.* **2021**, *2*, 603−624.

(9) Grenthe, I.; Ferri, D.; Salvatore, F.; Riccio, G. Studies on metal carbonate equilibria. Part 10. A solubility study of the complex formation in the uranium(VI)−water−carbon dioxide (g) system at 25 °C. *J. Chem. Soc., Dalton Trans.* **1984**, *11*, 2439−2443.

(10) Henglein, A.; Spinks, J. W. T. R. J. Woods: An Introduction to Radiation Chemistry, Third Edition, John-Wiley and Sons, Inc., New York, Toronto 1990. ISBN 0-471-61403-3. 574 Seiten, Preis: DM 91, 45. *Ber. Bunsenges. Phys. Chem.* **1991**, *95*, 451−451.

(11) Le Caër, S. Water Radiolysis: Influence of Oxide Surfaces on H2 Production under Ionizing Radiation. *Water* **2011**, *3*, 235−253.

(12) Richter, H. W. Radiation Chemistry: Principles and Applications. In *Photochemistry and Radiation Chemistry*; American Chemical Society, 1998; Vol. *254*, ch. 2, pp 5−33.

(13) Ekeroth, E.; Roth, O.; Jonsson, M. The relative impact of radiolysis products in radiation induced oxidative dissolution of UO_2. *J. Nucl. Mater.* **2006**, *355*, 38−46.

(14) Hiroki, A.; Laverne, J. A. Decomposition of hydrogen peroxide at water-ceramic oxide interfaces. *J. Phys. Chem. B* **2005**, *109*, 3364−3370.

(15) Barreiro Fidalgo, A.; Kumagai, Y.; Jonsson, M. The role of surface-bound hydroxyl radicals in the reaction between H_2O_2 and UO_2. *J. Coord. Chem.* **2018**, *71*, 1799−1807.

(16) Pablo, J. D.; Casas, I.; Clarens, F.; Aamrani, F. E.; Rovira, M. The Effect of Hydrogen Peroxide Concentration on the Oxidative Dissolution of Unirradiated Uranium Dioxide. In *MRS Online Proc. Libr.*; Materials Research Society, 2000; Vol. *663*, DOI: 10.1557/proc-663-409.

(17) Maier, A. C.; Kegler, P.; Klinkenberg, M.; Baena, A.; Finkeldei, S.; Brandt, F.; Jonsson, M. On the change in UO_2 redox reactivity as a function of H2O2 exposure. *Dalton Trans.* **2020**, *49*, 1241−1248.

(18) Zanonato, P. L.; Di Bernardo, P.; Grenthe, I. Chemical equilibria in the binary and ternary uranyl(vi)−hydroxide−peroxide systems. *Dalton Trans.* **2012**, *41*, 3380−3386.

(19) Li, J.; Szabó, Z.; Jonsson, M. Meta-studtite stability in aqueous solutions. Impact of HCO3−, H2O2 and ionizing radiation on dissolution and speciation. *Dalton Trans.* **2021**, *50*, 6568−6577.

(20) Zanonato, P. L.; Di Bernardo, P.; Szabó, Z.; Grenthe, I. Chemical equilibria in the uranyl(vi)−peroxide−carbonate system; identification of precursors for the formation of poly-peroxometallates. *Dalton Trans.* **2012**, *41*, 11635.

(21) Scholz, F.; Kahlert, H. Acid−Base Equilibria. In *Chemical Equilibria in Analytical Chemistry*; Springer International Publishing, 2019; pp 17−91.

(22) Perrin, D. D. Tables. In *Ionisation Constants of Inorganic Acids and Bases in Aqueous Solution*; *Elsevier*, 1982; pp 1 −138.

(23) Watanabe, T.; Ikeda, Y. A Study on Identification of Uranyl Complexes in Aqueous Solutions Containing Carbonate Ion and Hydrogen Peroxide. *Energy Procedia* **2013**, *39*, 81−95.

(24) Chung, D.-Y.; Park, M.-S.; Lee, K.-Y.; Lee, E.-H.; Kim, K.-W.; Moon, J.-K. Decomposition of uranyl peroxo-carbonato complex ion in the presence of metal oxides in carbonate media. *J. Radioanal. Nucl. Chem.* **2015**, *306*, 761−768.

(25) Puigdomènech, I.; Colàs, E.; Grivé, M.; Campos, I.; García, D. A tool to draw chemical equilibrium diagrams using SIT: Applications to geochemical systems and radionuclide solubility. *MRS Online Proc. Libr.* **2014**, *1665*, 111−116.

(26) Kressin, I. K. Spectrophotometric method for the determination of uranium in urine. *Anal. Chem.* **1984**, *56*, 2269−2271.

(27) Savvin, S. Analytical use of arsenazo III Determination of thorium, zirconium, uranium and rare earth elements. *Talanta* **1961**, *8*, 673−685.

(28) Ghormley, J. A.; Stewart, A. C. Effects of γ-Radiation on Ice1. *J. Am. Chem. Soc.* **1956**, *78*, 2934−2939.

(29) Li, Q.; Sritharathikhun, P.; Motomizu, S. Development of Novel Reagent for Hantzsch Reaction for the Determination of Formaldehyde by Spectrophotometry and Fluorometry. *Anal. Sci.* **2007**, *23*, 413−417.

(30) Lousada, C. M.; Jonsson, M. Kinetics, Mechanism, and Activation Energy of H2O2 Decomposition on the Surface of ZrO2. *J. Phys. Chem. C* **2010**, *114*, 11202−11208.

(31) Maier, A. C.; Iglebaek, E. H.; Jonsson, M. Confirming the Formation of Hydroxyl Radicals in the Catalytic Decomposition of H_2O_2 on Metal Oxides Using Coumarin as a Probe. *ChemCatChem* **2019**, *11*, 5435−5438.

(32) Yang, M.; Soroka, I.; Jonsson, M. Exploring the limitations of the Hantzsch method used for quantification of hydroxyl radicals in systems of relevance for interfacial radiation chemistry. *Radiat. Phys. Chem.* **2017**, *130*, 1−4.

(33) Yang, M.; Jonsson, M. Surface reactivity of hydroxyl radicals formed upon catalytic decomposition of H2O2 on ZrO2. *J. Mol. Catal. A: Chem.* **2015**, *400*, 49−55.

(34) Shiraishi, H.; Kataoka, M.; Morita, Y.; Umemoto, J. Interactions of Hydroxyl Radicals with Tris (Hydroxymethyl) Aminomethane and Good's Buffers Containing Hydroxymethyl or Hydroxyethyl Residues Produce Formaldehyde. *Free Radical Res. Commun.* **1993**, *19*, 315−321.